AMERICAN SOCIETY FOR MICROBIOLOGY | Applied and Environmental Microbiology

Silver Nanoparticles Decrease the Viability of *Cryptosporidium parvum* Oocysts

Pamela Cameron,[b,d] Birgit K. Gaiser,[c] Bidha Bhandari,[a] Paul M. Bartley,[b] Frank Katzer,[b] Helen Bridle[a]

Heriot-Watt University, School of Engineering, Edinburgh, United Kingdom[a]; Moredun Research Institute, Penicuik, United Kingdom[b]; Heriot-Watt University, School of Life Sciences, Nanosafety Research Group, Edinburgh, United Kingdom[c]; Novo Science Ltd., Edinburgh, United Kingdom[d]

Oocysts of the waterborne protozoan parasite *Cryptosporidium parvum* are highly resistant to chlorine disinfection. We show here that both silver nanoparticles (AgNPs) and silver ions significantly decrease oocyst viability, in a dose-dependent manner, between concentrations of 0.005 and 500 μg/ml, as assessed by an excystation assay and the shell/sporozoite ratio. For percent excystation, the results are statistically significant for 500 μg/ml of AgNPs, with reductions from 83% for the control to 33% with AgNPs. For Ag ions, the results were statistically significant at 500 and 5,000 μg/ml, but the percent excystation values were reduced only to 66 and 62%, respectively, from 86% for the control. The sporozoite/shell ratio was affected to a greater extent following AgNP exposure, presumably because sporozoites are destroyed by interaction with NPs. We also demonstrated via hyperspectral imaging that there is a dual mode of interaction, with Ag ions entering the oocyst and destroying the sporozoites while AgNPs interact with the cell wall and, at high concentrations, are able to fully break the oocyst wall.

Contaminated drinking water is one of the most important environmental contributors to the human and livestock disease burden, being responsible for an estimated 1.9 million human deaths each year, with protozoan parasites, such as *Cryptosporidium parvum*, being responsible for a significant proportion of this number (1). *C. parvum* is also of significant concern to farmers, as postmortem data indicate that the majority of calves who die at less than 1 month of age are infected with this parasite (2). Tap water is the most common risk factor for recorded human cases (3), since *Cryptosporidium* oocysts are robust and long-lived, have a low infectious dose, and are highly resistant to chlorination (4). The parasite is resistant to most commercial disinfectants, and while filtration can physically remove oocysts, this is not always available or completely effective. Recent research has concentrated on finding a means of inactivating the parasite, and *C. parvum* has previously shown sensitivity to oxidative stress induced by hydrogen peroxide. However, the extremely high concentration required (10% [vol/vol]) makes it impractical for widespread use (5).

Recently, numerous studies established that silver nanoparticles (AgNPs) are highly toxic to bacteria and fungi (6–9) and that this toxicity is often associated with ion release and induction of oxidative stress (7). Consequently, AgNPs are incorporated into consumer products, such as clothes made of AgNP-containing fabric (10) and personal hygiene products (11), primarily due to these antibacterial and antifungal properties. Others are incorporated into wound dressings (12), nano-silver toothpastes, and colloidal silver suspensions designed as nutritional supplements (13). Since *C. parvum* has previously shown sensitivity to oxidative stress, we sought to determine the effect of AgNPs on oocyst viability. At the time that we undertook our study, no previous work had investigated the impact of nanoparticles on waterborne protozoan pathogens. A recent article reported some degree of *C. parvum* oocyst inactivation upon exposure to AgNPs (14). Our work assesses the dose dependence of nanoparticle action on waterborne protozoan pathogens and additionally ascertains whether AgNPs have any effect on the viability of *C. parvum* oocysts and whether this effect is due to the presence of Ag ions, the nanoparticles, or a combination of both.

MATERIALS AND METHODS

Materials. *C. parvum* oocysts were obtained from the Creative Science Company (Penicuik, United Kingdom). The oocysts were of the Moredun isolate and were stored in phosphate-buffered saline (PBS) at 4°C. All experiments were performed within 4 months of oocyst preparation, and untreated control samples of identical age were used for comparison in every excystation assay. NM300 AgNPs were purchased from Mercator GmbH, and all other chemicals were from Sigma.

Particles and particle characterization. NM300 is one of the representative manufactured nanomaterials included in the OECD's Working Party on Manufactured Nanomaterials Sponsorship Programme and has therefore been chosen for investigation in an increasing number of projects in order to allow comparison of data across multiple sources. It is a colloidal 10% (wt/wt) dispersion of AgNPs in water containing 4% (wt/wt) each of polyoxyethylene glycerol trioleate and Tween 20 (15). NM300 and the NP-free dispersant control, NM300-DIS, were obtained from Mercator GmbH, Germany. Characterization data for these AgNPs were obtained previously for the original suspension and for AgNPs in cell culture medium by transmission electron microscopy (TEM), dynamic light scattering (DLS), and inductively coupled plasma optical emission spectrometry (ICP-OES), as reported by Kermanizadeh et al. (16). NM300 is explicitly produced as a reference material to allow comparison between studies, and the same batch of material was used in this study.

In addition, NM300 NPs were characterized by DLS in sterile water at the exposure concentrations used for this study. For this purpose, NPs were sonicated for 8 min in sterile water in a sonicating water bath at a concentration of 5 mg/ml in a glass vial, followed by inversion of the vial

Received 28 August 2015 **Accepted** 12 October 2015

Accepted manuscript posted online 23 October 2015

Citation Cameron P, Gaiser BK, Bhandari B, Bartley PM, Katzer F, Bridle H. 2016. Silver nanoparticles decrease the viability of *Cryptosporidium parvum* oocysts. Appl Environ Microbiol 82:431–437. doi:10.1128/AEM.02806-15.

Editor: D. W. Schaffner

Address correspondence to Pamela Cameron, pam@novoscience.co.uk.

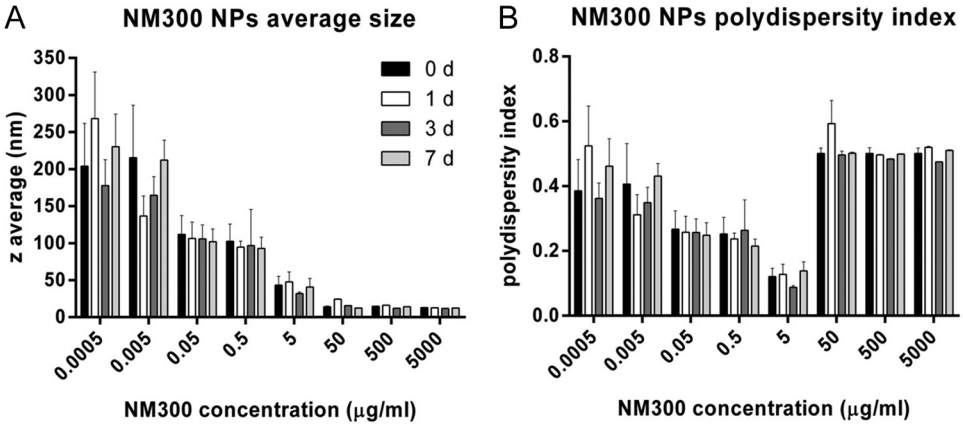

FIG 1 Z averages and polydispersity indexes for Ag nanoparticles suspended in sterile water over the concentration range used in this study and stability of suspensions over time (1, 3, and 7 days). Values are means and SEM for three individual experiments.

and a second sonication cycle. Serial dilutions of the suspensions were then examined by DLS according to the manufacturer's manual.

Nanoparticle preparation and exposures. For *in vitro* exposures, particle suspensions were prepared by sonication in a water bath twice for 8 min each in deionized water, as described above. Oocysts (final concentration, 1×10^6/ml) were incubated in sterile water (SLS) at room temperature with various concentrations of AgNPs for a maximum of 30 min. Viability was assessed visually by phase-contrast light microscopy for detection of intact oocysts.

Assessment of viability by excystation assay. Oocysts were incubated as described above and then immediately assessed for viability using the established excystation assay (17). Briefly, samples were incubated in the presence of trypsin (1% [wt/vol]; pH 3.0) at 37°C for 30 min. Samples were then centrifuged and the supernatant discarded before sodium deoxycholate (1% [wt/vol]) was added and samples were again incubated at 37°C for 40 min. Viability was assessed by counting the numbers of oocysts, sporozoites, and empty shells by phase-contrast microscopy and expressing the number of empty shells divided by the number of oocysts and empty shells as a percentage and thus a measure of excystation of the parasites. Each shell contains four sporozoites, so the sporozoite/empty shell ratio was also calculated.

The percent excystation was calculated by using the counted numbers of oocysts and empty shells with different concentrations of silver nanoparticles, as follows: % excystation = [(number of empty shells)/(number of oocysts + number of empty shells)] × 100. The sporozoite/shell ratio was calculated by using the counted numbers of empty shells and sporozoites, as follows: sporozoite/shell ratio = (number of sporozoites)/(number of empty shells).

Hyperspectral imaging. Oocyst and AgNP samples were sent to CytoViva Inc. (Auburn, AL). Samples were analyzed using an enhanced dark-field transmission optical microscope (Olympus BX43) equipped with a 100× objective and a hyperspectral imaging spectrophotometer (CytoViva Inc.). The spectrophotometer was used to record spectra with a low signal-to-noise ratio in visible and near-infrared wavelengths (400 to 1,000 nm) at a high spectral resolution (2.5 nm). Ten dark-current images were collected at the beginning of each hyperspectral image acquisition and were subtracted from the hyperspectral image data. A spectral classification algorithm (Spectral Angle Mapper) that uses an *n*-dimensional angle (equal to the number of wavelengths analyzed) was applied to match pixels on the hyperspectral image to reference libraries acquired by analyzing nanosilver samples dispersed in water.

Statistical analysis. All data are expressed as means ± standard errors of the means (SEM). Statistical analysis was performed by Student's *t* test (unpaired, two-tailed), using GraphPad Prism software (GraphPad Software, Inc.), and all data represent the means for at least three independent experiments. *P* values of <0.05 were deemed to be statistically significant.

RESULTS

Nanoparticle characterization. The results of the characterization performed in deionized water as part of this study are summarized in Fig. 1. At concentrations of 5 μg/ml and higher, the Z average, which describes the intensity-weighted harmonic mean size of the NPs, was in the "nano-range" of 100 nm and smaller, with no significant changes over a 7-day period (Fig. 1A). At the lowest concentrations, higher Z averages were found, which can likely be attributed to the relatively larger contribution of large dust particles as background noise.

The polydispersity index (pdi) gives an indication of agglomeration of particles in the suspension. The best-dispersed suspensions were present with concentrations between 0.05 and 5 μg/ml AgNPs, and at higher concentrations an increase in agglomeration to a pdi of approximately 0.5 was measured (Fig. 1B). At high concentrations of NPs, collisions between particles occur more frequently, and therefore agglomeration is encouraged. Similar to the Z average, the pdi remained stable over the 7-day time course. Despite the increase in polydispersity, the Z averages at the higher concentrations indicate good dispersion and a small average diameter, which may be due partly to larger agglomerates precipitating.

In addition to this information, Kermanizadeh et al. reported sizes of NM300 NPs as determined by X-ray diffraction of 7 nm (wet phase) and 14 nm (dried sample) and an average diameter of 17.5 nm as measured by TEM, with primary particle sizes ranging from 8 to 45 nm (16). Particles were mainly euhydral, with some elongated or subspherical morphologies present. AgNP dissolution in water was assessed at 1, 16, and 128 μg/ml over 24 h and was found to be $<0.01\%$, 0.78%, and 0.59%, respectively (16). Particles were assessed for endotoxin contamination and were endotoxin-free (data not shown).

Dose-dependent effect of silver nanoparticles on *C. parvum* oocyst integrity. Samples containing 1×10^6 *Cryptosporidium* oocysts were exposed to silver nanoparticle concentrations ranging from 5 ng/ml to 5 mg/ml. Three replicate experiments were performed for each concentration. After 30 min of nanoparticle incubation with each sample, the effect of the nanoparticles upon the oocysts was assessed visibly using phase-contrast microscopy. A clear AgNP concentration dependence was observed for oocyst destruction. Figure 2 shows typical images of samples following

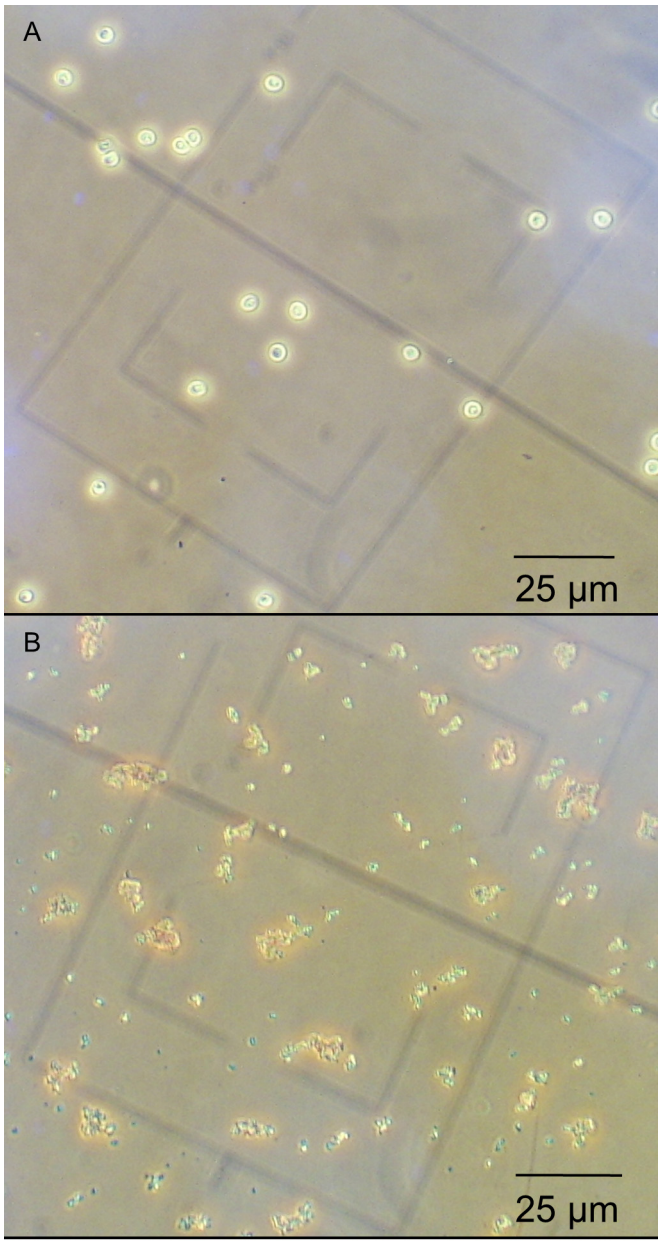

FIG 2 Effect of silver nanoparticles on *C. parvum* viability as assessed by phase-contrast light microscopy. Magnification, ×400. Viable intact oocysts (A) and nonviable oocysts/cell debris in the presence of AgNP (500 mg/ml) (B) are shown.

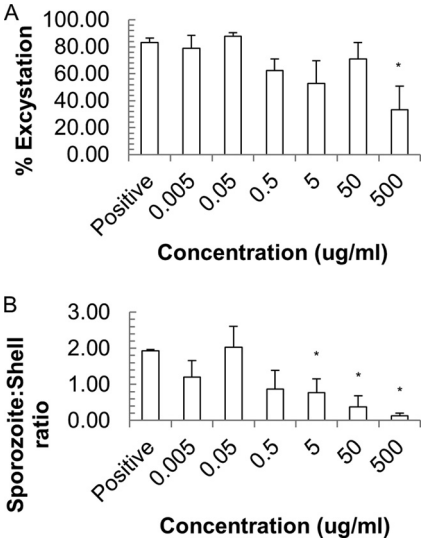

FIG 3 Effect of silver nanoparticles on *C. parvum* viability as assessed by % excystation (A) and the sporozoite/shell ratio (B). Values are means and SEM for three individual experiments. *, $P < 0.05$.

nanoparticle exposures at the highest concentration studied. These images indicate that silver nanoparticles induce oocyst death at high concentrations, leading to a breakup of the oocyst structure such that only debris is observed.

Dose-dependent effect of silver nanoparticles on excystation of *C. parvum* oocysts. While the above-described experiments indicated that high concentrations of nanoparticles were capable of destroying the oocyst outer wall, a further research question was whether the oocysts which remained intact also remained viable and infectious. Since oocysts cannot be cultured in the lab via traditional microbiological techniques, methods such as determining the MIC or minimum bactericidal concentration (MBC) cannot be utilized. Several methods have been developed to assess oocyst viability, although the gold standard remains the use of animal models, which are expensive and time-consuming and should be used with caution, as other assessment techniques could provide adequate data without requiring infectivity studies (17). An alternative marker of infectivity is the ability of oocysts to undergo excystation, the process by which oocysts rupture and release the sporozoites which initiate infection in host cells, as approved by The Drinking Water Inspectorate.

In the present study, an identical set of oocyst nanoparticle exposures was repeated, and the impact of the nanoparticles was assessed by excystation assay. Excystation was triggered using a standard protocol of exposure as described in Materials and Methods. The effect of nanoparticles on the viability of oocysts was analyzed through two measures of excystation: the percentage of excystation (Fig. 3A and Table 1) and the sporozoite/shell ratio (Fig. 3B and Table 1).

The results indicate very little change in percent excystation with increasing doses of AgNPs, although the highest AgNP concentration (500 μg/ml) caused significantly less sporozoite excystation, with a decrease from 83.3% ± 3% to 33.3% ± 17.5%. In contrast, the sporozoite/shell ratio decreased significantly as the amount of AgNPs added increased, with significant changes starting at 5 μg/ml ($P < 0.05$), most likely reflecting the toxicity of AgNPs to naked sporozoites.

Dose-dependent effect of silver ions on excystation of *C. parvum* oocysts. Samples containing 1×10^6 *Cryptosporidium* oocysts were exposed to silver ions at concentrations ranging from 0.0005 to 5,000 μg/ml. Three replicate experiments were performed for each concentration. As with the silver nanoparticles, the impacts of silver ions on viability and infectivity were assessed using excystation protocols. Again, percent excystation (Fig. 4A) and the sporozoite/shell ratio (Fig. 4B) were employed as means to determine the extent of excystation (Table 1). As with the AgNPs, significant effects on the excystation percentage were observed only at concentrations of 500 μg/ml and above. However, the

TABLE 1 Results of excystation protocols by both measures of excystation and with both AgNPs and Ag ions[a]

Ag state and concn (μg/ml)	% excystation	Sporozoite/shell ratio
AgNPs		
Control (no Ag)	83.33 ± 3.3	1.93 ± 0.03
0.005	79 ± 9.5	1.2 ± 0.46
0.05	88 ± 2.5	2.03 ± 0.58
0.5	62.33 ± 8.65	0.87 ± 0.52
5	53 ± 16.8	**0.77 ± 0.38**
50	71 ± 12.3	**0.38 ± 0.3**
500	**33.33 ± 17.5**	**0.13 ± 0.07**
Ag ions		
Control (no Ag)	85.67 ± 3.93	2 ± 0.4
0.0005	82.67 ± 3	1.2 ± 0.46
0.005	72.33 ± 13.5	1.37 ± 0.57
0.05	78 ± 9	1.97 ± 0.47
0.5	80 ± 8.5	1.55 ± 0.35
5	79.67 ± 7	1.47 ± 0.09
50	83.33 ± 2	1.5 ± 0.35
500	**66.33 ± 0.5**	**0.37 ± 0**
5,000	**62 ± 2.5**	**0.07 ± 0.03**

[a] Data are means ± SEM. Values in bold are statistically significant ($P < 0.05$).

sporozoite/shell ratio was not affected at lower concentrations, with the results for 5 μg/ml not being significantly different from those for the positive control. For higher concentrations, i.e., 500 μg/ml and above, it is clear that silver ions do reduce the sporozoite/shell ratio ($P < 0.05$).

Hyperspectral imaging. Enhanced dark-field hyperspectral microscopy is a technique which allows for the optical visualization and spectral characterization of nanosized objects. As a result, the location of silver nanoparticles can be determined (18–20). Enhanced dark-field microscopy enables detection of the scatter from silver nanoparticles at sizes below the optical microscopy resolution limit. Hyperspectral imaging of samples enables spectral characterization of silver nanoparticles based on their unique spectral characteristics. Figure 5 shows images of oocysts for comparison of the negative-control sample with one exposed to AgNPs; the latter clearly shows signs of obvious morphological changes, with such damage likely to mediate a loss of viability. Figure 6 shows the response of the reference AgNP sample as well as an image of an oocyst in the presence of AgNPs. Figure 6B shows an NP interacting with the oocyst wall, whereas internalization of AgNPs is not observed.

DISCUSSION

Recently, there has been considerable interest in the use of nanotechnology for water purification. In particular, the use of nanomaterials in small-scale, point-of-use or emergency response treatment systems has been proposed and investigated. For example, ceramic filters embedded with silver have been tested in several developing countries, and bactericidal silver nanoparticle paper was recently reported in *Environmental Science and Technology* (21). However, while it is known that certain nanoparticles exhibit antibacterial activity, only one other study has investigated the impact of nanoparticles on protozoa (14), also concentrating on *Cryptosporidium*, even though this pathogen is a leading cause of waterborne disease (1). The results presented here confirm that silver nanoparticles and silver ions are toxic to the waterborne protozoan pathogen *Cryptosporidium*, and they quantify the dose dependence of this effect.

Whether silver nanoparticle toxicity is due to particles, ions, or a combination of both has been hotly debated over the last decade, and many mechanisms of action have been proposed (e.g., see references 22 and 23). It is well known that AgNPs can be oxidized in aqueous solutions, leading to release of silver ions, and recent publications suggest that in the case of controlled aqueous laboratory media, AgNP toxicity is due to silver ion release into the exposure medium (9, 24, 25). However, this may vary in water containing high concentrations of chlorides or organic matter, which could form largely insoluble complexes with Ag ions and therefore reduce their toxicity (26).

A particular advantage of studying *Cryptosporidium* is that this pathogen offers a unique opportunity to gather deeper insight into the mechanisms of nanoparticle interaction with biological samples; in most cellular suspensions the halogen-containing culture medium precludes the accurate evaluation of silver ion toxicity, as silver halides tend to precipitate at low concentrations. Furthermore, nanoparticle properties, such as agglomeration and aggregation, surface charge, and adsorption of proteins, are generally highly dependent on the surrounding medium (e.g., see references 27 and 28). The robustness of *Cryptosporidium* oocysts enabled experiments to be conducted in water so that both the comparison of nanoparticles versus ions and the mechanisms of action of the particles in as close to their native state as possible in a solution could be investigated.

Recent work by Xiu et al. concluded that there was a negligible particle-specific antibacterial activity of silver nanoparticles, though organism-specific responses could lead to different observations in other biological systems (9). They found that antibacterial activity as a function of released silver ions from AgNPs was indistinguishable from that for the equivalent concentration of silver ions (from silver nitrate). However, we observed greater toxicity with AgNPs at equivalent concentrations, suggesting that the oocyst response to AgNPs differs from the bacterial response.

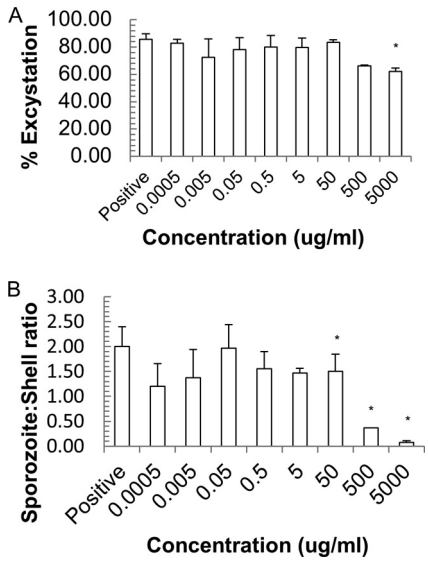

FIG 4 Effect of silver nitrate on *C. parvum* viability as assessed by % excystation (A) and the sporozoite/shell ratio (B). Values are means and SEM for three individual experiments. *, $P < 0.05$.

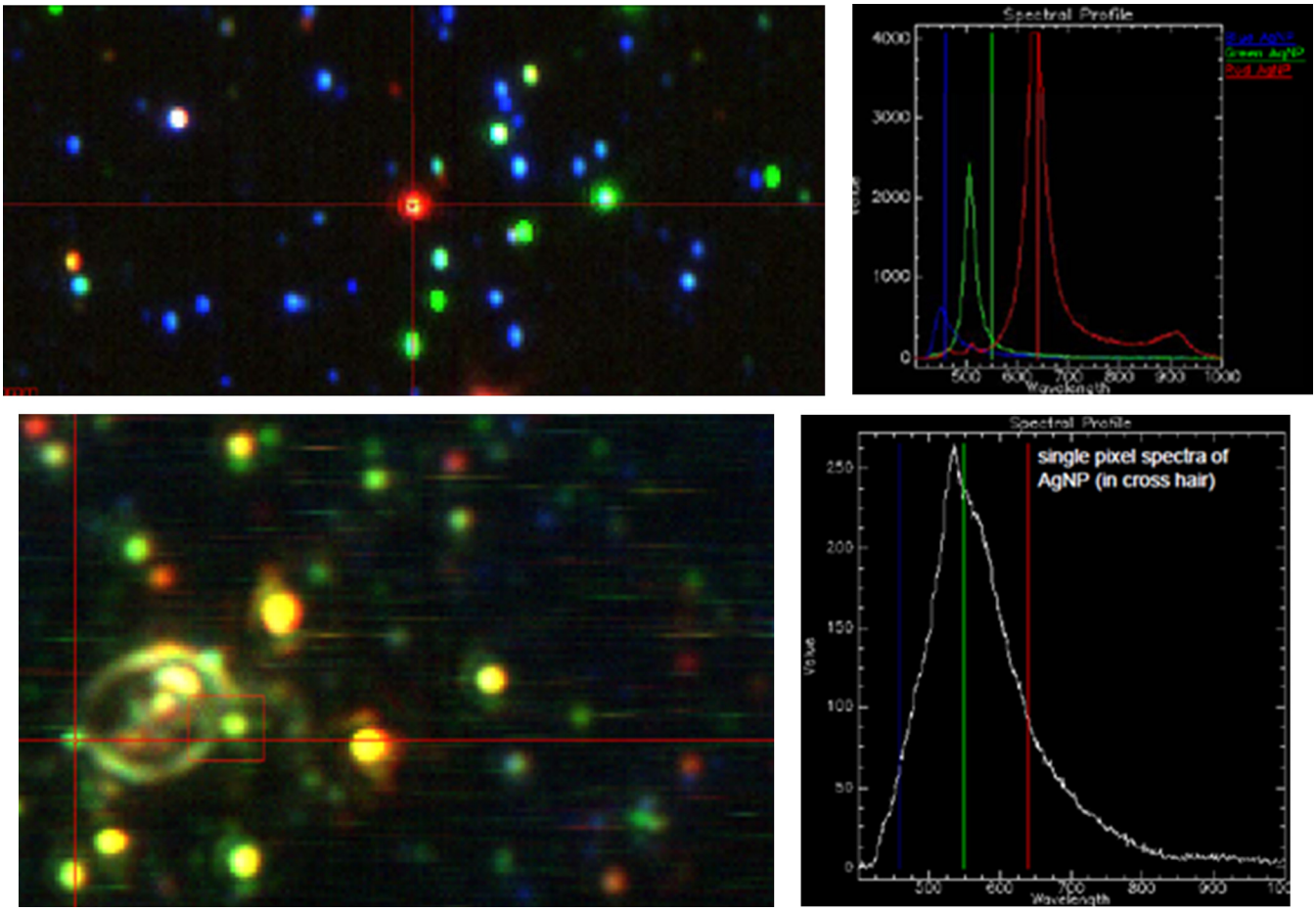

FIG 5 Hyperspectral imaging. (Top) Visualization of AgNPs via spectral imaging. NPs vary significantly in color, from blue (smallest) to red (largest), when illuminated with full-spectrum light due to the plasmon resonance effect. The left image shows a micrograph of a slide, whereas the right image shows the spectral profiles of different particles. (Bottom) Observation of NPs interacting with the oocyst wall. Again, the left image shows a micrograph image, specifically overlaid bright-field and spectral images, to show both the oocyst and the AgNPs. The right image shows the spectral profile of the highlighted green NP interacting with the oocyst wall.

Over a range of concentrations comparable to those observed for bacterial toxicity, both silver nanoparticles and silver ions were observed to either trigger destruction of the oocysts or render oocysts nonviable (Table 1). At the same microbial density, the MBCs for *Escherichia coli* and *Staphylococcus aureus* with AgNPs were reported to be 20 and 40 μg/ml, respectively (6). This is a factor of 10 lower than the results for *Cryptosporidium* by use of excystation percentage but a factor of 10 higher by use of the

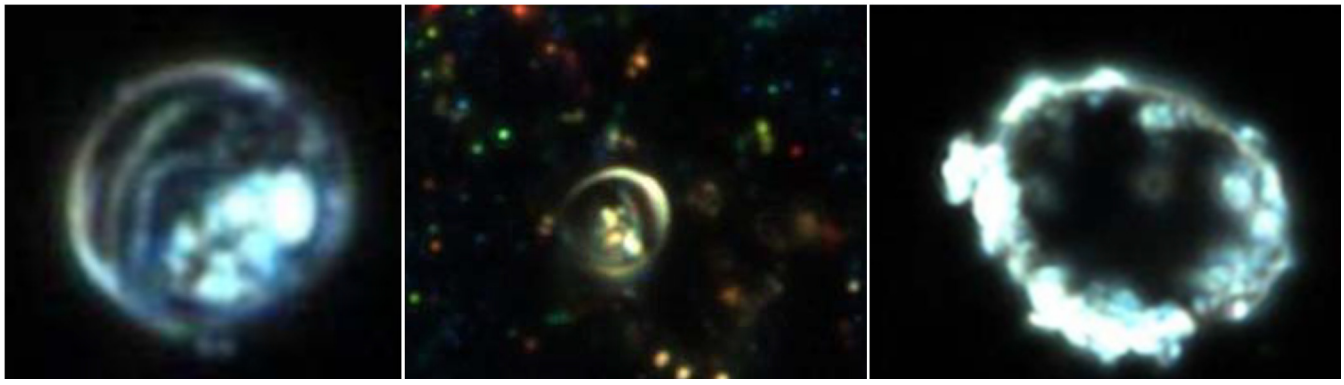

FIG 6 Hyperspectral imaging depicting the effect of silver NPs on *C. parvum*. (Left) Control, intact oocyst. (Middle) NPs added to the oocyst. (Right) Oocyst after 2 h of exposure to NPs, showing the observable impacts on the cell wall and interior.

sporozoite/shell ratio as a measure of viability. The same study found the MBC for these bacteria with silver ions to be 7.5 μg/ml (6), a factor of 100 lower than the results observed for *Cryptosporidium* with either measure of excystation. The result obtained with silver ions was as expected, since *Cryptosporidium* oocysts have a protective outer wall which, for example, resists disinfection by chlorine, to which bacteria are particularly susceptible. Given this robust outer wall, it was surprising to observe a toxicity of AgNPs similar to that for bacteria.

Additionally, while the bacterial study found silver ions to be more cytotoxic than AgNPs (6), our results indicate that AgNPs appear to be slightly more toxic than silver ions to oocysts. For example, the impact on excystation percentage became significant at the same concentration (500 μg/ml), with AgNPs leading to a greater reduction in excystation percentage (to 33% with AgNPs, compared to 62% with ions). Previous characterization of the NPs employed revealed that fewer than 1% of AgNPs dissolve in water (16), suggesting that the silver ion concentration equivalent to 500 μg/ml AgNPs is 5 μg/ml silver ions, further confirming our hypothesis that AgNPs are more toxic, as there was a clear impact of 500 μg/ml AgNPs, whereas no changes were observed with 5 μg/ml silver ions. Additionally, using the sporozoite/shell ratio as a measure, AgNP toxicity was noted at much lower concentrations than those for silver ions, most likely because sporozoites are more susceptible to NPs than oocysts are and therefore are more easily destroyed, reducing the observed ratio. Greater AgNP toxicity through the impact of the medium on silver ion bioavailability has been reported previously.

One previous study of oocyst exposures to AgNPs and ions was conducted by Su et al., who utilized 100 μg/ml of AgNPs and the equivalent concentration of Ag ions, i.e., 63.5 μg/ml of Ag ions (100 μg/ml of $AgNO_3$), with 4-h exposures (14). These concentrations were at the upper range of what we investigated, though our exposures took place over just 30 min. Su et al. reported excystation percentages of 42.7% for oocysts exposed to AgNPs, 71.4% for those treated with silver nitrate, and 89.5% for untreated oocysts, which are comparable to our results. Su et al. concluded that Ag ions were ineffective at inactivation of oocysts, implying that the impact of AgNP action was in some way related to an intrinsic property of the NP itself. This is also in agreement with our observation that AgNPs are more toxic than silver ions to oocysts. However, Su et al. did note that AgNP action was often attributed to the release of silver ions, though they offered no explanation for why little effect was observed with Ag in their results. We compared the influences of particles and ions by performing viability dose-response assays for each state of the material. Our findings indicate that while both AgNPs and Ag ions are capable of inactivation of *C. parvum* oocysts, there is a strong dose dependence, with AgNPs exhibiting greater toxicity.

The greater toxicity of AgNPs was more apparent depending upon the excystation measure e_Pmployed. The ratio of the number of oocysts to the number of shells (excystation percentage) might not reveal the influence of silver upon oocysts if the inactivation occurs through sporozoite destruction, as empty oocysts might still undergo excystation. However, by considering the sporozoite/shell ratio, this factor can be accounted for. Our results clearly indicated a decrease in the sporozoite/shell ratio with increasing silver doses, showing that exposure reduces oocyst viability through sporozoite destruction. This is in agreement with the findings of Su et al., who observed sporozoite destruction by phase-contrast imaging and the dielectrophoretic response (14). Sporozoite destruction suggests an internalization of silver nanoparticles or ions. Su et al. observed sporozoite destruction within intact oocysts, confirming that the wall was not destroyed, via propidium iodide staining. At high concentrations, we observed destruction of the oocyst wall, at which point it is reasonable to infer sporozoite destruction because sporozoites are much less robust than the oocyst itself, and indeed are packaged within the oocyst structure to protect them from the environment. Our results showed sporozoite/shell ratio decreases at much lower AgNP concentrations than those of silver ions (statistically significant effects noted at 5 μg/ml versus 500 μg/ml). One explanation is that the presence of AgNPs contributes to greater silver internalization, potentially mediated by the local low pH enhancing silver release following AgNP binding to the membrane, in an enhanced "Trojan horse" effect which has previously been suggested as a mechanism for nanoparticle toxicology after uptake into lysosomes (29). An alternative is that bound AgNPs are not removed before the excystation assay and thus remain a source of silver ions as sporozoites are excysted, although the results of Su et al. suggest the occurrence of sporozoite destruction before the oocyst wall is broken.

Hyperspectral imaging with enhanced dark-field microscopy offers a significantly higher signal-to-noise ratio and therefore better scatter detection of particles than conventional optical methods, and the spectral profiles of NPs can be used to detect NPs by hyperspectral imaging; this method has increasingly been used for the study of environmental samples (18, 19, 30), including the semiquantitative detection of uptake of NPs by protozoa (19) and the study of disinfection of water samples (31). We employed hyperspectral imaging to study both whether nanoparticles interact with the membrane and the oocyst morphology after exposure. These experiments enabled preliminary conclusions on the mode of nanoparticle action. Our results supported by hyperspectral imaging clearly highlight the interaction of silver nanoparticles with the oocyst wall. Previous work noted the accumulation of AgNPs on cell surfaces and the formation of "pits" (8). Taken together with our other findings, the data appear to indicate that interaction of AgNPs with the oocyst wall is a critical step in mediation of the toxic effects observed, resulting in greater toxicity than that with Ag ions alone.

In conclusion, we have provided a detailed characterization of silver nanoparticle and ion toxicity on protozoan pathogens, such as *Cryptosporidium*. Furthermore, dose-response experiments showed that high concentrations of nanoparticles and ions cause oocyst destruction, with lower concentrations affecting viability. Comparison of excystation percentages and sporozoite/shell ratios indicates a greater sensitivity of the sporozoites to silver, with AgNPs leading to more sporozoite destruction. This work has revealed that, for oocysts, there is a particle-specific mechanism imparting a greater toxicity of nanoparticles than that of ions. Additionally, the use of hyperspectral imaging allowed us to confirm the interactions of AgNPs with the oocyst membrane and to observe the subsequent oocyst disruption.

Protozoan pathogens are a major contributor to the waterborne disease burden, and this dose-dependent analysis of silver nanoparticle and silver ion impacts will be highly useful in assisting the application of these materials for oocyst disinfection. While improvements in efficacy are also required to achieve a truly effective disinfectant, this can perhaps be achieved by combina-

tion with other materials/reagents. However, as noted above, the presence of, e.g., other ions or organic components in a sample can have an impact on toxicity, and further investigations with finished and raw waters are required.

ACKNOWLEDGMENTS

We thank David G. E. Smith (Moredun Research Institute) and Vicki Stone (Heriot-Watt University) for the use of laboratory space and consumables. We also acknowledge Byron Cheatham and CytoViva for technical assistance and for undertaking the hyperspectral imaging experiments.

FUNDING INFORMATION

P.C., B.K.G., and H.B. acknowledge the Heriot-Watt Crucible training program, which inspired the initiation of this project and also provided financial support through a grant from the Heriot-Watt Crucible fund, and the EU FP7 project InLiveTox (grant NMP4-SL-2009-228789) for providing the NM300 silver particles. P.M.B., P.C., and F.K. acknowledge Scottish government funding, and H.B. acknowledges the Royal Academy of Engineering/EPSRC for her research fellowship.

REFERENCES

1. **Striepen B.** 2013. Time to tackle cryptosporidiosis. Nature **503:**189–191. http://dx.doi.org/10.1038/503189a.
2. **Thomson S.** 2015. Cryptosporidiosis in farmed livestock. Ph.D. thesis. University of Glasgow, Glasgow, United Kingdom.
3. **Tam CC, Rodrigues LC, Viviani L, Dodds JP, Evan MR, Hunter PR, Gray JJ, Letley LH, Rait G, Tompkins DS, O'Brien SJ.** 2012. Longitudinal study of infectious intestinal disease in the UK (IID2 study): incidence in the community and presenting to general practice. Gut **61:**69–77. http://dx.doi.org/10.1136/gut.2011.238386.
4. **Rose JB, Huffman DE, Gennaccaro A.** 2002. Risk and control of waterborne cryptosporidiosis. FEMS Microbiol Rev **26:**113–123. http://dx.doi.org/10.1111/j.1574-6976.2002.tb00604.x.
5. **Barbee SL, Weber DJ, Sobsey MD, Rutala WA.** 1999. Inactivation of Cryptosporidium parvum oocyst infectivity by disinfection and sterilization processes. Gastrointest Endosc **49:**605–611. http://dx.doi.org/10.1016/S0016-5107(99)70389-5.
6. **Greulich C, Braun D, Peetsch A, Diendorf J, Siebers B, Epple M, Koller M.** 2012. The toxic effect of silver ions and silver nanoparticles towards bacteria and human cells occurs in the same concentration range. RSC Adv **2:**6981–6987. http://dx.doi.org/10.1039/c2ra20684f.
7. **Johnston HJ, Hutchison G, Christensen FM, Peters S, Hankin S, Stone V.** 2010. A review of the in vivo and in vitro toxicity of silver and gold particulates: particle attributes and biological mechanisms responsible for the observed toxicity. Crit Rev Toxicol **40:**328–346. http://dx.doi.org/10.3109/10408440903453074.
8. **Marambio-Jones C, Hoek EV.** 2010. A review of the antibacterial effects of silver nanomaterials and potential implications for human health and the environment. J Nanoparticle Res **12:**1531–1551. http://dx.doi.org/10.1007/s11051-010-9900-y.
9. **Xiu Z-M, Zhang Q-B, Puppala HL, Colvin VL, Alvarez PJJ.** 2012. Negligible particle-specific antibacterial activity of silver nanoparticles. Nano Lett **12:**4271–4275. http://dx.doi.org/10.1021/nl301934w.
10. **Kulthong K, Srisung S, Boonpavanitchakul K, Kangwansupamonkon W, Maniratanachote R.** 2010. Determination of silver nanoparticle release from antibacterial fabrics into artificial sweat. Part Fibre Toxicol **7:**8. http://dx.doi.org/10.1186/1743-8977-7-8.
11. **Chao JB, Liu JF, Yu SJ, Feng YD, Tan ZQ, Liu R, Yin YG.** 2011. Speciation analysis of silver nanoparticles and silver ions in antibacterial products and environmental waters via cloud point extraction-based separation. Anal Chem **83:**6875–6882. http://dx.doi.org/10.1021/ac201086a.
12. **Silver S, Phung Le T, Silver G.** 2006. Silver as biocides in burn and wound dressings and bacterial resistance to silver compounds. J Ind Microbiol Biotechnol **33:**627–634. http://dx.doi.org/10.1007/s10295-006-0139-7.
13. **Nowack B, Krug H, Height M.** 2011. 120 years of nanosilver history: implications for policy makers. Environ Sci Technol **45:**1177–1183. http://dx.doi.org/10.1021/es103316q.
14. **Su Y-H, Tsegaye M, Varhue W, Liao K-T, Abebe LS, Smith JA, Guerrant RL, Swami NS.** 2014. Quantitative dielectrophoretic tracking for characterization and separation of persistent subpopulations of Cryptosporidium parvum. Analyst **139:**66–73. http://dx.doi.org/10.1039/C3AN01810E.
15. **Comero S, Klein C, Stahlmecke B, Romazanov J, Kuhlbusch T, van Doren E, Wick P, Locoro G, Koerdel W, Gawlik B, Mast J, Krug HF, Hund-Rinke K, Friedrichs S, Maier G, Werner J, Linsinger T.** 2011. NM-300 silver characterisation, stability, homogeneity. JRC publication no. JRC60709 EUR 24693 EN. Publications Office of the European Union, Luxembourg, Luxembourg. http://dx.doi.org/10.2788/23079.
16. **Kermanizadeh A, Pojana G, Gaiser BK, Birkedal R, Bilanicova D, Wallin H, Jensen KA, Sellergren B, Hutchison GR, Marcomini A, Stone V.** 2013. In vitro assessment of engineered nanomaterials using a hepatocyte cell line: cytotoxicity, pro-inflammatory cytokines and functional markers. Nanotoxicology **7:**301–313. http://dx.doi.org/10.3109/17435390.2011.653416.
17. **Robertson LJ, Gjerde BK.** 2007. Cryptosporidium oocysts: challenging adversaries? Trends Parasitol **23:**344–347. http://dx.doi.org/10.1016/j.pt.2007.06.002.
18. **Beach J.** 2009. Hyperspectral imaging. BioOpt World **3:**2–4.
19. **Mortimer M, Gogos A, Bartolomé N, Kahru A, Bucheli TD, Slaveykova VI.** 2014. Potential of hyperspectral imaging microscopy for semi-quantitative analysis of nanoparticle uptake by protozoa. Environ Sci Technol **48:**8760–8767. http://dx.doi.org/10.1021/es500898j.
20. **Pratsinis A, Hervella P, Leroux J-C, Pratsinis SE, Sotiriou GA.** 2013. Toxicity of silver nanoparticles in macrophages. Small **9:**2576–2584. http://dx.doi.org/10.1002/smll.201202120.
21. **Dankovich TA, Gray DG.** 2011. Bactericidal paper impregnated with silver nanoparticles for point-of-use water treatment. Environ Sci Technol **45:**1992–1998. http://dx.doi.org/10.1021/es103302t.
22. **Ivask A, Kaweeteerawat EAC, Boren D, Fischer H, Ji Z, Chang CH, Liu R, Tolaymat T, Telesca D, Zink JI, Cohen Y, Holden PA, Godwin HA.** 2014. Toxicity mechanisms in Escherichia coli vary for silver nanoparticles and differ from ionic silver. ACS Nano **28:**374–386. http://dx.doi.org/10.1021/nn4044047.
23. **Yang X, Gondikas AP, Marinakos SM, Auffan M, Liu J, Hsu-Kim H, Meyer JN.** 2012. Mechanism of silver nanoparticle toxicity is dependent on dissolved silver and surface coating in Caenorhabditis elegans. Environ Sci Technol **46:**1119–1127. http://dx.doi.org/10.1021/es202417t.
24. **Gomes SIL, Soares AMVM, Scott-Fordsmand JJ, Amorim MJB.** 2013. Mechanisms of response to silver nanoparticles on Enchytraeus albidus (Oligochaeta): survival, reproduction and gene expression profile. J Hazard Mater **254–255:**336–344. http://dx.doi.org/10.1016/j.jhazmat.2013.04.005.
25. **Hoheisel SM, Diamond S, Mount D.** 2012. Comparison of nanosilver and ionic silver toxicity in Daphnia magna and Pimephales promelas. Environ Toxicol Chem **31:**2557–2563. http://dx.doi.org/10.1002/etc.1978.
26. **Fabrega J, Luoma SN, Tyler CR, Galloway TS, Lead JR.** 2011. Silver nanoparticles: behaviour and effects in the aquatic environment. Environ Int **37:**517–531. http://dx.doi.org/10.1016/j.envint.2010.10.012.
27. **Behra R, Sigg L, Clift MJ, Herzog F, Minghetti M, Johnston B, Petri-Fink A, Rothen-Rutishauser B.** 2013. Bioavailability of silver nanoparticles and ions: from a chemical and biochemical perspective. J R Soc Interface **10:**20130396. http://dx.doi.org/10.1098/rsif.2013.0396.
28. **Topuz E, Sigg L, Talinli I.** 2014. A systematic evaluation of agglomeration of Ag and TiO_2 nanoparticles under freshwater relevant conditions. Environ Pollut **193:**37–44. http://dx.doi.org/10.1016/j.envpol.2014.05.029.
29. **Sabella S, Carney RP, Brunetti V, Malvindi MA, Al-Juffali N, Vecchio G, Janes SM, Bakr OM, Cingolani R, Stellacci F, Pompa PP.** 2014. A general mechanism for intracellular toxicity of metal-containing nanoparticles. Nanoscale **6:**7052–7061. http://dx.doi.org/10.1039/c4nr01234h.
30. **Badireddy AR, Wiesner MR, Liu J.** 2012. Detection, characterization, and abundance of engineered nanoparticles in complex waters by hyperspectral imagery with enhanced darkfield microscopy. Environ Sci Technol **46:**10081–10088. http://dx.doi.org/10.1021/es204140s.
31. **Sankar MU, Aigal S, Maliyekkal SM, Chaudhary A, Anshup Kumar AA, Chaudhari K, Pradeep T.** 2013. Biopolymer-reinforced synthetic granular nanocomposites for affordable point-of-use water purification. Proc Natl Acad Sci U S A **110:**8459–8464. http://dx.doi.org/10.1073/pnas.1220222110.